Formation of Poly(propylene)-Based Biocomposite Films and Their Use in the Attachment of Methylene Blue

Jesica A. Cavallo, Cesar G. Gomez, Miriam C. Strumia*

Biocomposite PP-*g*-PAAc-CS films based on PP were generated and utilized as support of methylene blue, a thiazidic dye. Using a photograft polymerization of acrylic acid, the PP film was functionalized with carboxyl groups (PP-*g*-PAAc), which attached chitosan by electrostatic bond. A longer poly(acrylic acid) chain or a higher CS immobilization temperature led to a higher chain interpenetration and crosslinking reaction. Immobilized MB confirmed to possess redox activity from its reaction with ascorbic acid, where the dye decomposition rate (R'_d) increases together with the chain interpenetration, then decreasing with the increase in the crosslinking degree.

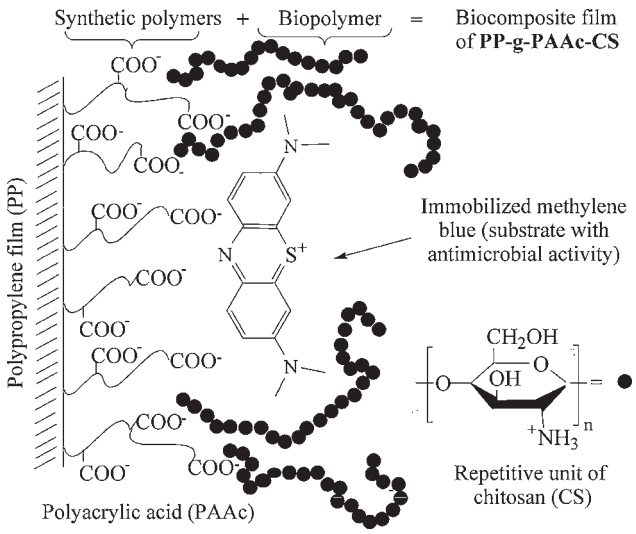

Introduction

The synthesis of biocomposite materials obtained from the combination of a natural and a synthetic polymer is being broadly studied, since this type of material displays interesting properties.[1–4] The conjunction of both polymers type enhances the properties of the final material, broadening its application field.[5–7] Biocomposite materials have proved useful in such varied fields as biomedical materials,[8] controlled-delivery systems,[9] biological tissue engineering, and food packaging.[5,8] The biopolymer "chitosan" (CS) is a polysaccharide chemically composed of linkages β-(1,4)-2-amino-2-deoxy-D-glucose attained from the deacetylation of chitin, an abundant biopolymer present in the shell of shrimps, crabs, and crawfish.[10] CS shows attractive properties such as biocompatibility, biodegradability, and antimicrobial activity, particularly useful in biomedical material and vegetable conservation.[11] Moreover, a synthetic polymer-like poly(propylene) (PP) has been widely used due to its mechanical properties, chemical resistance, and ability to be a barrier for certain gases. Since this polymer is not a biocompatible or a biodegradable material,[12] several modification reactions have taken place on PP in order to improve its properties;[13] the photograft polymerization being a method worth highlighting.[14]

On the other hand, methylene blue (MB) is a thiazidic dye used since the late nineteenth century in much biomedical research, and was considered a leading compound in clinical areas, including therapeutics for malaria and

J. A. Cavallo, C. G. Gomez, M. C. Strumia
Departamento de Química Orgánica, Facultad de Ciencias Químicas (IMBIV-CONICET),
Universidad Nacional de Córdoba, Edificio de Ciencias II, Haya de la Torre y Medina
Allende, 5000 Córdoba, Argentina
Fax: +54 351 433 4170 Ext. 150; E-mail: mcs@fcq.unc.edu.ar

DOI: 10.1002/macp.201000047

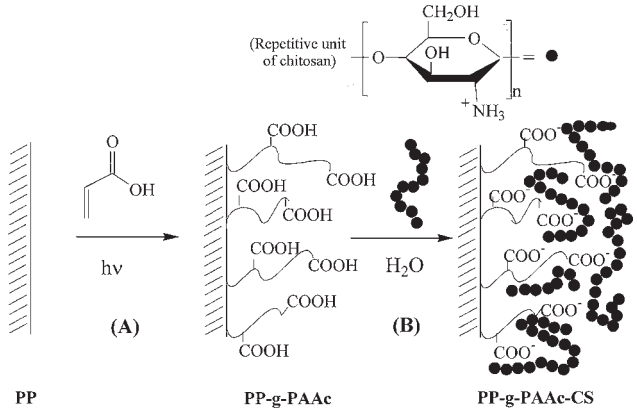

Scheme 1. Photograft polymerization of AAc onto the PP film surface (A), attaching the CS chains onto carboxylic groups through electrostatic bond (B).

schizophrenia.[15] The photodynamic therapy of cancer, and more recently of microbial infection (photodynamic antimicrobial chemotherapy), has also employed MB and its congeners, among other chemical types, due to their low human toxicity and efficient photosensitizing properties.[16] Therefore, this work aimed at attaining biocomposite films based on PP and modified with CS as support of MB. First, the PP film was functionalized with carboxyl groups from acrylic acid (AAc) photograft polymerization (Scheme 1), and then CS was immobilized through electrostatic bond to the film grafted with poly(acrylic acid) (PAAc), PP-*g*-PAAc, obtaining the biocomposite film (PP-*g*-PAAc-CS). We were interested in finding a product with the best properties for being used as a biomedical material or in food packaging. Since the antimicrobial activity of MB depends on its redox activity, the performance of the immobilized dye as an oxidizing agent was investigated in a heterogeneous system.

Experimental Part

Reagents and Equipment

The reagents were used as purchased. CS ($C_{12}H_{24}N_2O_9$) was obtained from Aldrich, USA. Isotactic PP film with a thickness of 20 μm was kindly supplied by Converflex S.A., Argentina. The crystallinity degree (48%) was determined from the melting endotherm of the polymer measured with a Perkin-Elmer Pyris DSC calorimeter at a heating rate of 10 °C · min^{-1}, assuming that the enthalpy of 100% crystalline isotactic PP is 138 J · g^{-1}. AAc (Merck, Germany) was purified by distillation under reduced pressure. Propionic acid (p.a., Fluka, Switzerland) and benzophenone (BP, p.a., Mallinckrodt, USA) were recrystallized by decreasing the temperature from a methanolic solution. Acetic acid and ascorbic acid were obtained in p.a. grade from Cicarelli, Argentina, MB (p.a.) from Anedra, Argentina. Spectrophotometric measurements were recorded on a spectrophotometer "MultiSpec-1501" Shimadzu, Japan. Fourier-transform infrared (FTIR) spectra of the samples were recorded on a Nicolet 5-SXC spectrometer (USA). Thermogravimetric analysis (TGA) and the mechanical properties of the films were performed on an analyzer Perkin-Elmer TGA 7 (Germany), and a rheometer Rheoplus/32-Physica MCR 301 "Anton Paar" (Switzerland), respectively. Scanning electron microscopy (SEM) was performed on a Phillips SEM 501 B instrument (Holland), at the Instituto Nacional de Tecnología Industrial (INTI), Córdoba, Argentina.

Photograft Polymerization of AAc onto PP Films

The surface of the PP film was initially modified with AAc using photograft polymerization at room temperature, BP as a radical initiator, and different reaction times. A PP film with a surface area of 64 cm^2 was weighed and immersed into a Petri capsule with 1.0 mL of AAc/H_2O 50% by volume solution. This mixture was then irradiated under ultraviolet-visible light using a medium pressure UV lamp (Engenlhard, Hanovia) and a nitrogen atmosphere at room temperature. Subsequently, the modified film was washed once with a NaOH aqueous solution at pH = 8 in order to remove the homopolymer and the reagent unreacted. Finally, the grafted film was washed exhaustively with distilled water and dried under reduced pressure. The reaction yield was expressed as the PAAc grafting degree (*G*), calculated using

$$G(\text{wt.}-\%) = \left(1 - \frac{\text{PP}}{\text{PP} - \text{g} - \text{PAAc}}\right) \times 100 \quad (1)$$

Chitosan Immobilization on PAAc-Grafted Films

CS was solubilized by addition of a 2 wt.-% acetic acid solution under stirring at room temperature, using a 1:1 molar ratio of amine to carboxyl groups. The final concentration of the aqueous CS solution was adjusted at 1 wt.-% with distilled water, reaching a pH value close to 5.5. This polymer (45 mL) was immobilized by electrostatic interaction between its ammonium groups and the carboxylate groups of the film grafted with PAAc for 4 h at room temperature. The CS-modified films were afterwards washed exhaustively in a beaker with distilled water under stirring at room temperature, and dried subsequently. The reaction of CS immobilization occurred by using films with different grafting degrees (*G* %) and temperature reactions. The degree of CS immobilization (*I*) was calculated according to:

$$I(\text{wt.}-\%) = \left(1 - \frac{\text{PP}-g-\text{AAc}}{\text{PP}-g-\text{PAAc} - \text{CS}}\right) \times 100 \quad (2)$$

Attachment of Methylene Blue to the Modified Films

The molecular structure of MB encloses a positive charge, which allows its fixation to the film grafted with PAAc through electrostatic interaction with the carboxylate groups of the PAAc polymeric chain, immobilizing the CS polymer in other similar stepways. Here, the film grafted with PAAc (near 0.030 g) was left in

Macromolecular Journals
DOI: 10.1002/macp.201000047

contact with 80 mL of a 4×10^{-5} M aqueous solution of MB at pH = 5.5 for 8 h at room temperature. The film was then exhaustively washed with distilled water in order to eliminate the dye unattached. Finally, the CS was immobilized to the films modified with MB using the procedure detailed in the previous section.

Swelling Degree of the Films

The swelling study of the samples was performed in water from a parameter denominated "equilibrium water content" (S_w) defined in Equation (3), δ_1 being the water density. The film was left in distilled water at pH = 5.7 during 24 h at room temperature, and then dried. Swollen (W_s) and dry mass (W_d) were measured before and after the drying step:

$$S_w(\text{mL/g}) = \frac{1}{\delta_1}\left(\frac{W_s}{W_d} - 1\right) \quad (3)$$

Results and Discussion

This study focused on the preparation of a biocomposite film containing appropriate properties for being used as a biomedical material or in packaging food. Biocomposite films (PP-*g*-PAAc-CS) were prepared from an AAc photograft polymerization, and CS was then conjugated to the film grafted with PAAc through electrostatic interaction in aqueous solution at pH = 5.5. During the AAc photograft polymerization, the time reaction was varied in order to obtain different degrees of grafting (*G*). Its effect on the CS immobilization reaction was analyzed and the final properties of the biocomposite films were attained. The characterization of the products was carried out through FTIR, thermal gravimetric analysis (TGA), mechanical properties, SEM, and water-swelling analysis. Moreover, MB was conjugated to the modified films between the layer of PAAc-grafted chains and that of CS, where the ability of the dye as a redox agent was examined in a heterogeneous system. One of our working hypotheses relied on the fact that the performance of the reaction between the immobilized dye and ascorbic acid in the aqueous solution depends on the diffusion of the latter, through the layers of PAAc-grafted/immobilized-CS. This phenomenon might provide additional information on the structural arrangement attained (chain interpenetration degree) between the PAAc-CS chains in the biocomposite films, determined by the length of PAAc-grafted chain. Therefore, the "structural arrangement of chains" controls the ascorbic acid diffusion and then its ability to react with the immobilized MB.

AAc-Photograft Polymerization onto PP Film

The photograft polymerization of PAAc onto PP films is carried out using a batch system, where the radical initiator

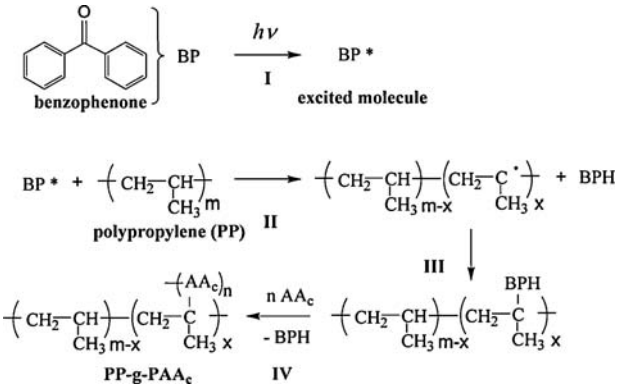

Scheme 2. Mechanism proposed for photograft polymerization of AAc onto the superficial polymeric backbones of PP.

BP incorporated into the reaction mixture is activated under the UV-light effect, as seen in Scheme 2. The activated BP is incorporated into the PP chain, which is subsequently substituted by addition of AAc. Figure 1 shows a typical curve of grafting degree (*G*) with an S-shaped in dependence on the time. After an induction period close to 15 min, characterized by a comparatively low grafting degree, which increases rapidly and an acceleration of the grafting reaction from 20 to 50 min is noticed in the intermediate stage. After a reaction time of about 50 min, the grafting rate decreases and the reaction yield levels off.[17] The active sites on the film surface increase with the reaction time, encouraging the onset, and development of the AAc photograft polymerization onto the PP film. However, a so long time of exhibition under the lamp light escorts to a higher surface degradation, where oxides of low molecular weight are generated. This factor contributes to beginning the AAc homopolymerization in the reaction mixture, which slows down the grafting reaction.[18]

In a study similar to the above described, the photograft reaction of AAc and propionic acid on PP films was carried

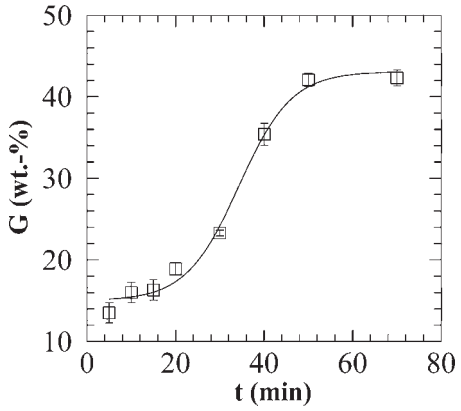

Figure 1. Influence of the irradiation time on AAc photograft polymerization, when a 0.2 M BP solution was used at room temperature. Nonlinear regression (sigmoidal).

Table 1. Variation of the grafting degree (*G*) as a function of the reaction time.

t	*A*	*G*	BPC[a)]	*D*[b)]	*L*
min	cm^2	%	wt.-%	$mol \cdot cm^{-2}$	
10	64	16	1.9	1.6×10^{-06}	19
20	64	19	2.3	2.0×10^{-06}	23
40	64	35	1.9	1.6×10^{-06}	51

[a)]Content of benzophenone (BPC) attached onto PP film is defined as BPC = 100 × (PP-BP − PP)/PP; [b)]Grafting density (*D*) is calculated as $D = (\text{PP-BP} - \text{PP})/(A \times M_{BP})$, where *A* is the film surface area and M_{BP} is the molecular weight of BP.[19]

out to demonstrate that the *G* value increases together with the chain length of PAAc. Since the molecular structure of propionic acid does not contain a double bond, this molecule cannot substitute the attached BP as found with AAc in pathway IV (Scheme 2). In this process the BP conjugation to the film surface takes place, where the BP content (BPC) attached to PP is obtained by gravimetric technique (Table 1). Assuming that BPC is directly related to the grafting density per surface area unit (*D*), and using the specific content of PAAc [(PP-*g*-PAAc − PP)/PP], the PAAc chain length (*L*) can be estimated as in Equation (4). Here, the $\overline{M}_w$ value corresponds to the molecular weight of the reagents, where NaAAc is the repetitive unit of the PAAc-grafted chain in its form of sodium salt.[19]

$$L = \frac{(\text{PP}-g-\text{AAc} - \text{PP})\overline{M}_w^{\text{BP}}}{(\text{PP}-g-\text{BP} - \text{PP})\overline{M}_w^{\text{NaAAc}}} \quad (4)$$

Table 1 shows that the *G* value increases faster for a reaction time longer than 20 min, while the BPC parameter displays a similar value. Moreover, the grafting density (*D*) value does not present a considerable variation when *G* increases (Table 1), supporting the hypothesis that a film grafted is attained with a longer PAAc backbone (*L*).

Immobilization Reaction of Chitosan onto PAAc-Modified Films

The immobilization reaction of CS was carried out through electrostatic interactions between the ammonium group of the polysaccharide and the carboxylic groups of the film grafted with PAAc (Scheme 1). In this work, the influence of different immobilization conditions such as grafting degree (*G*) and temperature reaction was investigated. Figure 2 displays the degree of CS immobilization (*I*) as a function of the PAAc grafting degree (*G*), where it is found that *I* value increases substantially together with *G* up to 19%. Afterwards, the curve remains constant since this reaction depends on the carboxylic group content. This behavior is related to the fact that the first chains of CS immobilized to the PAAc-modified film obstruct the attachment of new CS backbones by charge repulsion.[20] These results allow assuming the theory of the generation of well-defined layers, where the construction of stratified levels on the modified film surface is controlled by the length of the PAAc-grafted chain. Figure 3 exhibits the influence of temperature on the CS immobilization performance of films modified with *G* = 16 and 19%. It is observed that this variable affects mainly the *I* value of the films with *G* = 19%, which shows the influence of the PAAc-grafted chain length on the reaction of CS immobilization. In addition, until a maximum temperature of 65 °C, the film grafted with *G* = 19% displays a yield higher than that with *G* = 16% (Table 1), since a longer polymeric chain in the former leads

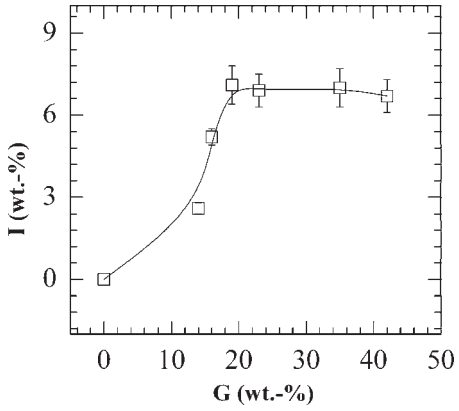

Figure 2. Degree of CS immobilization (%) as a function of the grafting degree (smoothing line), when a 1 wt.-% CS aqueous solution was left in contact with a PAAc-grafted film for 4 h at room temperature.

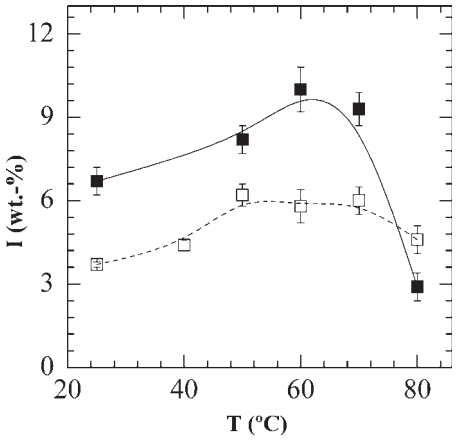

Figure 3. Effect of the reaction temperature on the CS immobilization degree, employing films grafted with *G* = 16 (white squares) and 19% (black squares), and a 1 wt.-% CS solution for 4 h of reaction. Both curves show smoothing line.

DOI: 10.1002/macp.201000047

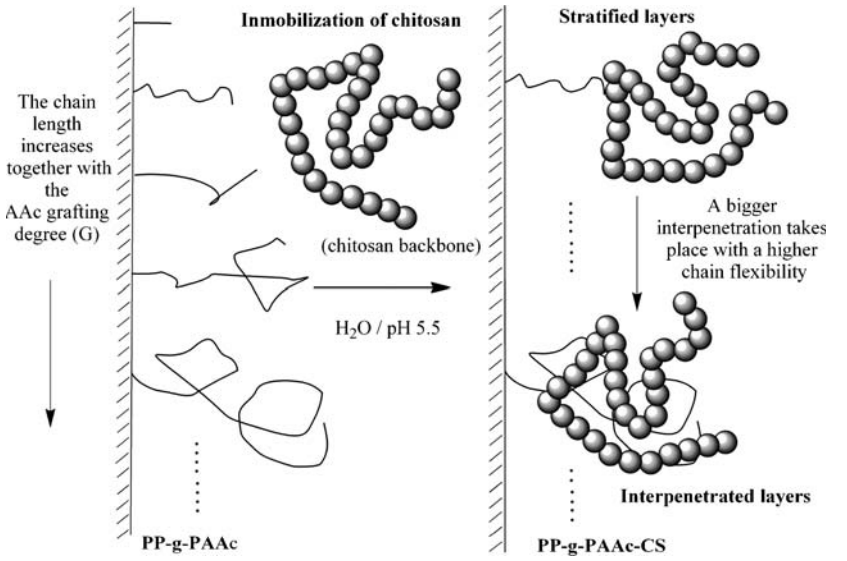

Scheme 3. Effect of PAAc-grafted chain length on the CS immobilization reaction and chain crosslinking degree.

to a greater backbone flexibility (Scheme 3). Figure 3 also shows that the rise in temperature favors a higher mobility of PAAc-grafted chain, both *I* curves exhibiting a maximum value of about 60 °C. Beyond this temperature, the chain interpenetration reaction gets an important yield. This phenomenon produces no covalent crosslinking between the chains, which reduces their mobility and ability to attach new CS chains (Scheme 3). Therefore, strong evidence suggests that the system reaches a higher degree of layer stratification when a shorter PAAc-grafted chain length is used in the CS immobilization reaction.

Characterization of the PP Films

FTIR Spectroscopy

The chemical composition of the PP films was analyzed using FTIR spectroscopy, where the chemical modification of the film in each reaction pathway could be demonstrated. The more important bands in the initial PP film are attributed to the C–H stretching vibration at 2 925 cm^{-1}, and to the C–H deformation vibration at 1 470 and 1 250 cm^{-1} (Figure 4). The film of PP-*g*-PAAc shows a new band at 1 710 cm^{-1} corresponding to the C=O stretching vibration of the carboxyl group. Finally, the attachment of CS to modified films was confirmed through the appearance of a characteristic band at 1 560 cm^{-1} which corresponds to N–H deformation of the amino group in the PP-*g*-PAAc-CS film.

Viscoelastic Properties of the PP Films

Dynamic experiments were performed in the linear viscoelastic region, using a sweep of amplitude at 10 Hz angular frequency (ω) at 25 °C. Variation of the tensile stress (σ) as function of the deformation (ε) was investigated, by which the elastic modulus (E') from the curve slope in the lineal viscoelastic range was estimated. Young's modulus (E') is a parameter that exhibits the stiffness performance of the film assayed. Figure 5 illustrates the variation of elastic modulus (E') of the films as a function of grafting degree (G) attained. It is seen that the AAc photograft polymerization carried out onto the initial PP increases the E' value of the resulting grafted film regarding the unmodified PP (Figure 5). This behavior may be mostly attributed to the fact that PP chain scission dominates the UV irradiation, and these short chains tend to reorganize themselves into crystalline structure.[21] A higher crystallinity reinforces the load value of the material, which exhibits a higher E' value. Although an atactic polymer such as the PAAc-grafted backbones has to contain a low crystallinity, its contribution to the elastic modulus should not be discarded, because their carboxyl groups promote the formation of hydrogen bonds that cause the arrangement of a stable elastic network.[22] Figure 5 also shows that the film with $G = 19\%$ yields the highest elastic modulus measured, which is attributed to the fact that a further irradiation time results in a lower E' value since the photochemical degradation becomes significant. Although this technique provides functionality to the polymer surface and involves the initiation of vinyl monomer polymerization from reactive sites generated on the film surface,[19,23] the degradation reactions occurring during grafting have to be avoided. Therefore, as the film with $G = 16\%$ exhibited the better

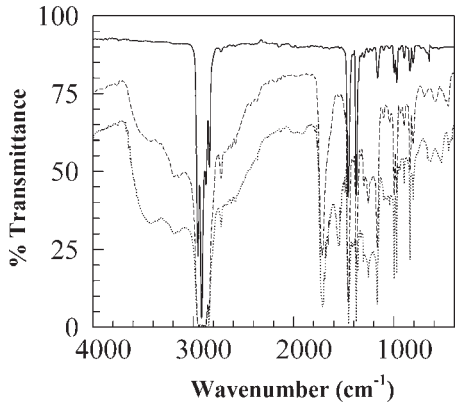

Figure 4. FTIR spectra corresponding to different PP films. Initial PP (continuous line), PP-*g*-PAAc with $G = 16\%$ (dash line) and PP-*g*-PAAc-CS with $G = 16\%$ and $I = 2.7\%$ (dotted line).

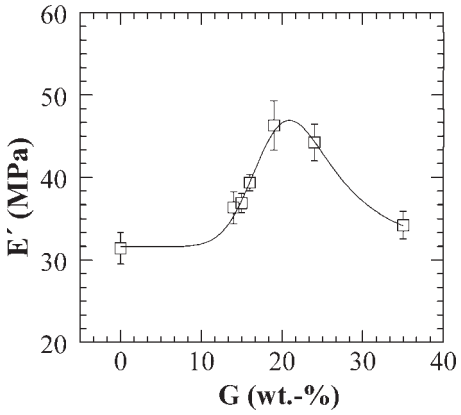

Figure 5. Elastic modulus (*E'*) of films modified (PP-*g*-PAAc) against the grafting degree (*G*) of the samples measured in dry state. Nonlinear regression (exponentially modified Gaussian peak function).

mechanical properties, it was selected as a good candidate for carrying out the study of CS immobilization. In addition, Figure 6 shows an interesting behavior of the elastic modulus corresponding to the films modified with CS (PP-*g*-PAAc-CS). Although the *E'* value decreases when a higher temperature of CS immobilization is used, the former exhibits a degree of stiffness higher than that found in the initial PP and PAAc-grafted films (Figure 5). During the drying process the segments of CS as well as the PAAc-grafted chains are progressively ordered until the film reaches its dry state, where crystalline regions appear in the CS layer of the CS-modified film (PP-*g*-PAAc-CS). These crystalline areas increase their resistance to deformation, which must be related to the generation of an additional interaction, such as the hydrogen bond between the amino groups of the CS chains. This bond contributes to the growth of new crystalline domains; the final material is also strengthened. In Figure 6 it can be seen that when a higher reaction temperature is used during the CS immobilization, the modulus *E'* of the CS-modified films decreases until attaining a similar value to that found in the PAAc-grafted film with $G = 16\%$ (PP-*g*-PAAc). Clearly, chain flexibility increases in conjunction with temperature, leading to a higher interpenetration degree between the polymeric chains of PAAc and CS. This behavior demonstrates that the crystalline domain decreases, which can be observed from the decreasing *E'* value (Figure 6). In addition, it should be noted that the decrease of the crystallinity in the PP-*g*-PAAc-CS films depends largely on the CS layer, since the lowest *E'* value attained by the system is similar to that found in the PP-*g*-PAAc film with $G = 16\%$ (Figure 5 and 6). The results obtained from the analysis of the mechanical properties of the films confirmed the generation of layers with different degrees of structural arrangement during CS immobilization when different temperatures were used.

TGA of the Films

This testing procedure is applied to samples to measure variations in weight in relation to changes in temperature. Such analysis relies on three high precision measurements: weight, temperature, and temperature change. Figure 7 illustrates the mass variation of the modified films as a function of the temperature applied, where the initial PP film begins its decomposition from 300 °C, showing 100 wt.-% mass loss at 400 °C. Nevertheless, Figure 7 reveals that a slight degradation at 200 °C takes place in the PP-*g*-PAAc and PP-*g*-PAAc-CS films, reaching a weight loss near 10% when the materials are kept at 400 °C. The curve of thermal decomposition that each product shows against the temperature signals that the modification reaction took place in the initial PP film, displaying a noticeable increase

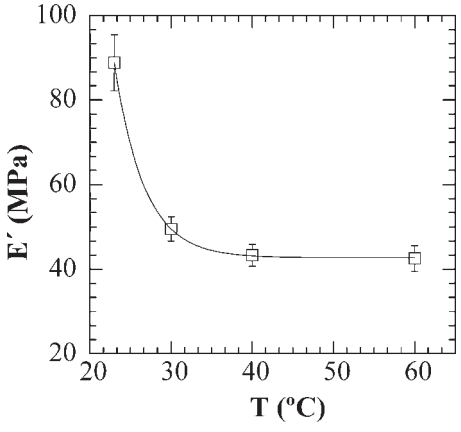

Figure 6. Elastic modulus (*E'*) of dry products of PP-*g*-PAAc-CS attained from the CS immobilization to PAAc-grafted films ($G = 16\%$) at different reaction temperatures. Nonlinear regression (exponential decay 1).

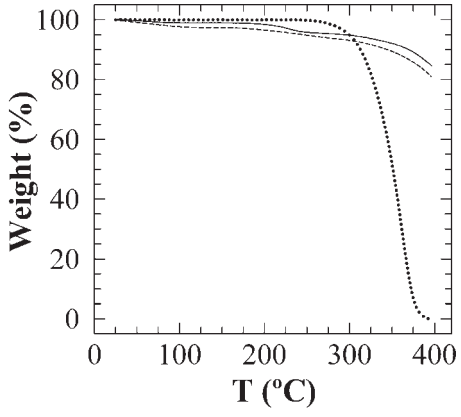

Figure 7. Thermogravimetric assays of the samples carried out at nitrogen atmosphere using a flow of 80 mL · s^{-1} and a temperature slope of 10 °C · min^{-1}. Initial PP (dotted line), PP-*g*-PAAc with $G = 16\%$ (continuous line) and PP-*g*-PAAc-CS film with $G = 16\%$ and $I = 2.7\%$ (dash line).

DOI: 10.1002/macp.201000047

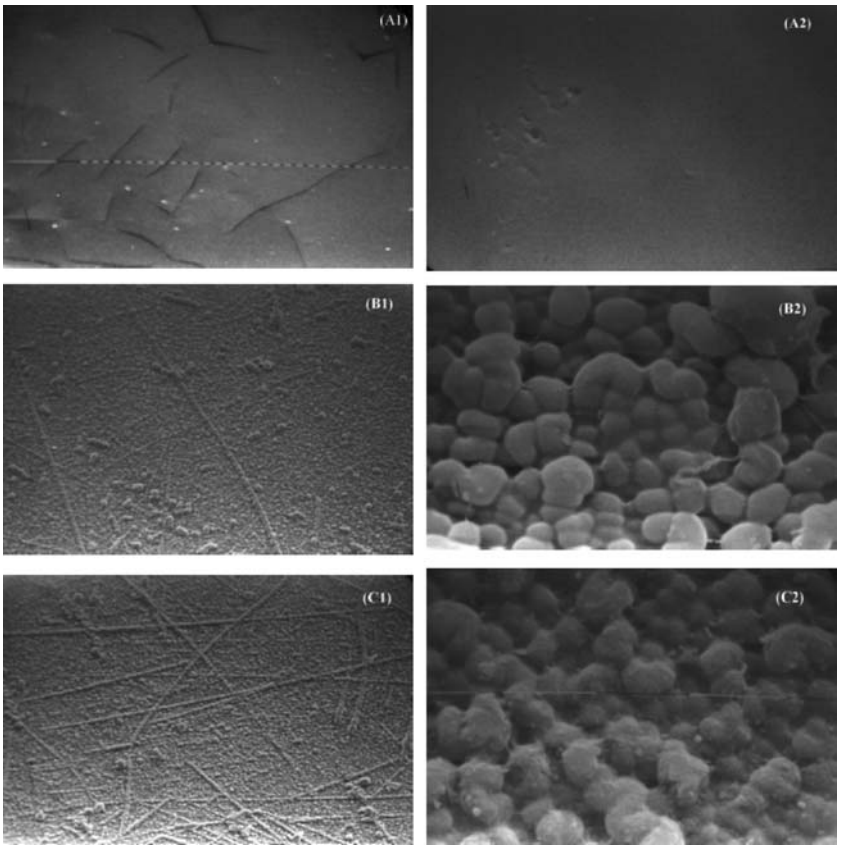

Figure 8. SEM of initial PP surface (A), film grafted ($G = 16\%$) with PAAc (B), and biocomposite film (PP-*g*-AAc-CS) with $G = 16\%$ and $I = 3.6\%$ (C). Micrographs were obtained using magnifications of 160× (1) and 2 500× (2).

in thermal stability. This behavior is closely associated with the incorporation of the PAAc-grafted chains in the film. A dehydration process occurs near 200 °C, where two carboxyl groups from the same or adjacent chains undergo cyclization and lead to an anhydride structure of higher thermal stability.[21]

SEM

The morphologic characterization of the film in its dry state through SEM corroborated the existence of a marked difference between the initial PP and the PP-*g*-PAAc film, which confirmed that the AAc-photograft polymerization had taken place (Figure 8). Here, the unmodified PP film displays a smooth surface, while the surface of the PAAc-grafted film forms granules as deriving from its chain arrangement. Figure 8 also shows that, once the immobilization reaction of CS has taken place, the surface of the PP-*g*-PAAc-CS product exhibits granules with borderlines less defined than those found in the PAAc-grafted film. This behavior relates to the fact that the interpenetration between the chains of both polymers increases chain disorder in the PAAc-grafted/CS layers of the product obtained.

Swelling of the Modified Films

The swelling study of the modified films was carried out in distilled water using the parameter S_w [Equation (3)] referred to as "equilibrium water content." Figure 9 shows that the S_w value of the PP-*g*-PAAc and PP-*g*-PAAc-CS films has a performance similar to that seen in the curve of Figure 2, since their swelling degree depends on the content of the hydrophilic group. However, the S_w curve corresponding to the PP-*g*-PAAc films grows steeper than that found in the PP-*g*-PAAc-CS films (Figure 9), the former achieving the highest S_w value near 25 *G* %. Although the ammonium group displays a hydrophilic character, the S_w value of the PP-*g*-PAAc-CS films increases slightly up to $G = 19\%$. For CS-modified films with a grafting degree higher 19%, the S_w value is noticeably lower than that found in PP-*g*-PAAc films (Figure 9). This behavior supports the claim described in the Section "Immobilization Reaction of Chitosan onto PAAc-Modified Films", where the interpenetration and crosslinking reactions of CS take place mostly from a minimum PAAc-grafted chain length (close to $G = 20\%$). Since flexibility is determined by the length of the polymeric chain, a longer PAAc-grafted chain results in a higher mobility, the polymeric backbone of CS subsequently yielding a higher interpenetration degree (Scheme 3). The increase in the entanglements and crosslinking points decreases the

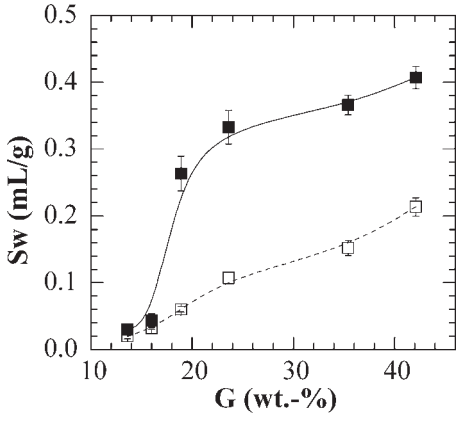

Figure 9. Equilibrium water content (S_w) of films grafted with PAAc (black square) and biocomposite films (white square) as a function of the grafting degree. Both curves show smoothing line.

stretching ability of the chain in the interpenetrated layers of both polymers, the biocomposite film then decreases its capacity to regain water. Figure 10 indicates that the S_w performance corresponding to PP-*g*-PAAc-CS films with $G = 16$ and 19% produces a different response against the temperature of CS immobilization, making evident the effect of the PAAc-grafted chain length on the reaction. This figure also shows that the S_w curve of the film with $G = 19\%$ exhibits a noticeable change against temperature. The S_w parameter initially increases with temperature up to 65 °C, where the curve achieves its maximum value. This pattern is attributed to the fact that a higher thermal energy gives rise to an increased conformational freedom of PAAc chain and a higher immobilization degree of hydrophilic CS-chains. When the temperature of CS-immobilization reaction and the PAAc chain flexibility are high enough, the interpenetration extent becomes important, yielding a higher degree of chain crosslinking and a lower swelling capacity.

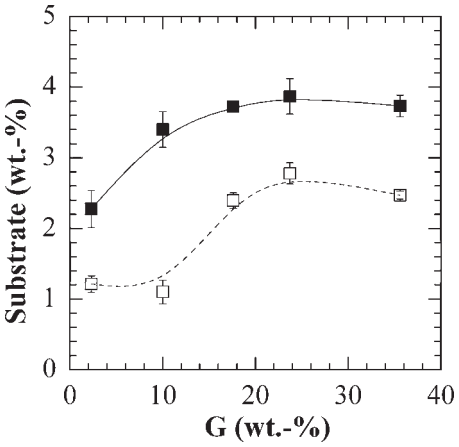

Figure 11. Attachment of MB (black square) to films grafted with PAAc using different grafting degrees at room temperature. CS was then immobilized (white squares) to dye-modified films by electrostatic interaction. Smoothing line was utilized in both cases.

Reaction Performance of Methylene Blue Immobilized on the Modified Films

The chain structural arrangement reached between the layers of PAAc and CS built on the film surface was examined, using a spectrophotometric method based on the ascorbic acid diffusion and its ability to react with MB supported in the bilayer of biocomposite films. MB was anchored onto PAAc-modified films with different grafting degrees at room temperature, and CS was then immobilized. Figure 11 shows that the content of the dye attached reaches its maximum value from a film with $G = 10\%$ keeping constant, which exhibits the effect of electrostatic repulsion from the first positive charges joined at the surface. The chains of CS in another pathway were then immobilized to the above dye-modified films, also by electrostatic interaction. Figure 11 shows that, although the *I* curve presents a tendency similar to that found in Figure 4, the new *I* values are lower than those reported above. This performance arises from the fact that the dye molecules have already occupied a fraction of the total negative charges, while the yield of the CS immobilization is controlled mainly by the length (or flexibility) of the PAAc-grafted chain.

Finally, a 0.1 M ascorbic acid aqueous solution (2.5 mL) was left at room temperature in contact with the biocomposite film containing MB, using a molar ratio ascorbic acid to MB of 100. Figure 12 shows the kinetics of

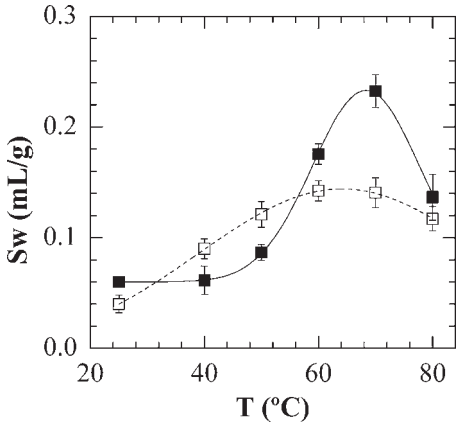

Figure 10. Equilibrium water content (S_w) of biocomposite films attained from the CS immobilization to films grafted with $G = 16$ (white squares, nonlinear regression, Gaussian function) and 19% (black squares, smoothing line was used to link data) at different reaction temperatures.

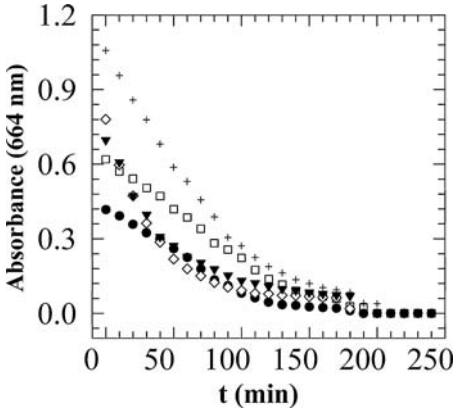

Figure 12. Reaction kinetics between MB supported into modified films and a 0.1 M ascorbic acid aqueous solution at room temperature. The biocomposite films used to support MB had $G = 2$ (black spheres), 10 (white squares), 16 (crosses), 24 (white diamonds), and 36% (black triangles). The dye content was monitored by UV-Vis spectroscopy measuring absorbance at 664 nm.

DOI: 10.1002/macp.201000047

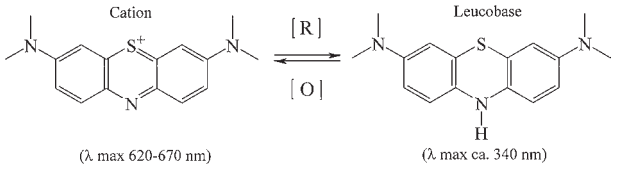

Scheme 4. Oxidized and reduced form of MB present in a redox reaction.

oxide reduction between ascorbic acid in solution and MB immobilized to biocomposite films as a function of time. From the absorbance measurement at 664 nm by UV-vis spectroscopy, the decrease in the content of the oxidized dye was assayed (Scheme 4). This demonstrates that immobilized MB maintains its redox activity, from which the presence of antimicrobial activity on the film surface can be expected. The figure also indicates that the curve linear range of the biocomposite films with a higher G value would show a more pronounced slope, which is associated with a faster "decomposition rate of the dye" (R'_d). Since the value of the slope is directly related to decomposition rate ($R'_d \sim d_{Abs.}{}^{664\ nm}/dt$) and also depends on the ascorbic acid diffusion through the bilayer of PAAc and CS, the structural arrangement of the chains can be inferred. It would seem that a higher diffusion of ascorbic acid is linked to a lower layer stratification provided by a higher degree of chain interpenetration (Scheme 3), where each polymer exhibits a high structural disorder of backbones. Figure 13 evidences that the value of R'_d increases in conjunction with $G \approx 25\%$, and then decreases. Although a longer PAAc-grafted chain leads to a higher chain interpenetration rate and solute diffusion, when the former is large enough (beyond 25%), the chain crosslinking degree becomes significant, which generates a mesh with a high crosslinking density; the diffusion of ascorbic acid thus decreases. Clearly, the length of PAAc-grafted chain has determined the chain

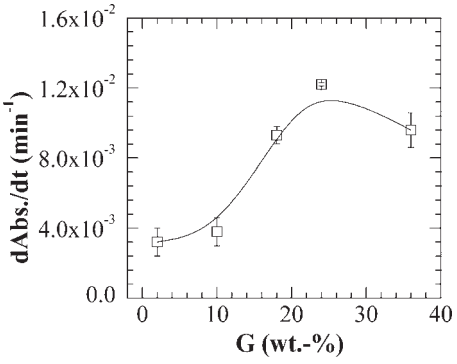

Figure 13. Decomposition rate ($R'_d \sim d_{Abs.}^{664nm}/dt$) of MB immobilized to biocomposite films containing different grafting degrees, where the reaction between the dye and ascorbic acid depends on the chain structural arrangement of the bilayer PAAc-CS (smoothing line).

flexibility, which influences the interpenetration reaction and structural arrangement of the polymeric chains in each layer.

Conclusion

The formation of biocomposite films based on PP was analyzed in order to obtain new materials as support of a substrate such as MB with redox activity. The PP film was superficially modified through AAc photograft polymerization, where time and temperature reactions were examined. The carboxyl groups of PAAc-grafted films were then used to be attached to CS by electrostatic interaction, studying the influence of PAAc chain length, and temperature reactions on the final properties of the biocomposite films attained. These products were characterized by FTIR, TGA, mechanical properties, and their swelling degree. Although a longer time of photograft polymerization involves a higher G value and a longer PAAc-grafted chain, a G value higher than 19% corresponds to films modified with a higher level of degradation. This behavior was corroborated from the mechanical properties of the films modified with PAAc, where the elastic modulus decreases when the grafting degree increases, as a longer degradation reaction of the film is produced. However, the grafting reaction provides the PAAc-modified films with an elastic modulus higher than that found in the initial PP. This phenomenon has been attributed to the fact that during photograft polymerization, PP chain scission also occurs, where these short backbones tend to reorganize themselves into crystalline structures. A further increase in the elastic modulus is provided by the CS immobilization to films grafted with PAAc. The CS chain displays hydrogen bond interaction, which increases crystalline domains. Since the CS interpenetration reaction becomes more important with a longer PAAc chain, the crystallinity of the bilayer PAAc-CS decreases and a lower elastic modulus is observed. A similar behavior is found with the increase in the CS immobilization temperature, leading to a higher CS interpenetration degree, and a decrease in the crystallinity of the products. In addition, films grafted with PAAc beyond $G = 19\%$ showed a swelling degree significantly greater than that found in films modified with CS, which reveals the increase of the interpenetration reaction and chain crosslinking degree. Moreover, the structural arrangement of the bilayer PAAc-CS was investigated from the reaction performance between ascorbic acid and MB supported in the modified films, where the oxide-reduction reaction was controlled by ascorbic acid diffusion. It was found that MB immobilized to biocomposite films maintains its redox activity, inferring the existence of antimicrobial activity on the film surface. Additionally, the dye decomposition rate increases together with the length of PAAc-grafted chain up to $G = 25\%$, since a

higher chain interpenetration degree contributes to the disorder of the layers. A grafting degree beyond 25% leads to a higher chain crosslinking degree in biocomposite films (PP-*g*-PAAc-CS), decreasing the solute diffusion and achieving a lower R'_d. The chain interpenetration rate is significant from a minimum PAAc chain length (close to $G = 20\%$), and has a considerable influence on the structural organization of the backbones in each layer, and in the diffusion of ascorbic acid.

Acknowledgements: The authors thank *CONICET*, *FONCYT*, and *SECYT-UNC* for their financial support, as well as language assistance by *Carolina Mosconi*.

Received: January 26, 2010; Revised: April 15, 2010; Published online: DOI: 10.1002/macp.201000047

Keywords: biomaterials; chitosan; methylene blue; packaging; poly(propylene) (PP)

[1] E. Gunister, D. Pestreli, C. H. Unlu, O. Aticib, N. Gungor, *Carbohydr. Polym.* **2007**, *67*, 358.
[2] Y. Li, Y. Umasankar, S. M. Chen, *Anal. Biochem.* **2009**, *388*, 288.
[3] L. Avérous, P. J. Halley, *Biofuels, Bioprod. Biorefin.* **2009**, *3*, 329.
[4] Y. Chen, C. Liu, P. R. Chang, D. P. Anderson, M. A. Huneault, *Polym. Eng. Sci.* **2009**, *49*, 369.
[5] N. T. Dai, M. K. Yeh, C. H. Chiang, K. C. Chen, T. H. Liu, A. C. Feng, L. L. Chao, C. M. Shih, H. K. Sytwu, S. L. Chen, T. M. Tim-Mo Chen, E. F. Adams, *Biochem. Biophys. Res. Commun.* **2009**, *386*, 21.
[6] Z. Zhong, X. S. Sun, D. Wang, *J. Appl. Polym. Sci.* **2007**, *103*, 2261.
[7] T. W. Xu, J. H. Xu, W. Yu, J. H. Zhong, *Biotechnol. J.* **2006**, *1*, 1293.
[8] J. Jagur-Grodzinski, *Polym. Adv. Technol.* **2006**, *17*, 395.
[9] Z. Hou, Q. Sun, Q. Wang, J. Han, Y. Wang, Q. Zhang, *Drug Dev. Res.* **2009**, *70*, 206.
[10] D. De Britto, O. B. G. De Assis, *Int. J. Biol. Macromol.* **2007**, *41*, 198.
[11] M. Ye, H. Neetoo, H. Chen, *Food Microbiol.* **2008**, *25*, 260.
[12] A. Neamnark, N. Sanchavanakit, P. Pavasant, T. Bunaprasert, P. Supaphol, R. Rujiravanit, *Carbohydr. Polym.* **2007**, *68*, 166.
[13] M. Z. Elsabee, E. S. Abdou, K. S. A. Nagy, M. Eweis, *Carbohydr. Polym.* **2008**, *71*, 187.
[14] A. Bhattacharya, B. N. Misra, *Prog. Polym. Sci.* **2004**, *29*, 767.
[15] M. Wainwright, H. Mohr, W. H. Walker, *J. Photochem. Photobiol. B: Biol.* **2007**, *86*, 45.
[16] M. Wainwright, *Photodiagn. Photodyn. Ther.* **2005**, *2*, 263.
[17] S. Francis, B. R. Dhanawade, D. Mitra, L. Varshney, S. Sabharwal, *Radiat. Phys. Chem.* **2009**, *78*, 42.
[18] J. Lei, X. Liao, *Eur. Polym. J.* **2001**, *37*, 771.
[19] H. Ma, R. H. Davis, C. N. Bowman, *Macromolecules* **2000**, *33*, 331.
[20] M. Raposo, O. N. Oliveira, Jr., *Braz. J. Phys.* **1998**, *28*, 392.
[21] N. Anjum, B. Gupta, A. M. Riquet, *J. Appl. Polym. Sci.* **2006**, *101*, 772.
[22] J. L. De la Fuente, M. Wilhelm, H. W. Spiess, E. L. Madruga, M. Fernández-Garcia, M. L. Cerrada, *Polymer* **2005**, *46*, 4544.
[23] J. Deng, W. Yang, *Eur. Polym. J.* **2005**, *41*, 2685.

DOI: 10.1002/macp.201000047